Nicholls, P. (1974) *Biochim. Biophys. Acta 346*, 261-310.
O'Donnell, T. J., & Olson, A. J. (1981) *Comput. Graphics 15*, 133-142.
O'Reilly, J. E. (1973) *Biochim. Biophys. Acta 292*, 509-515.
Pettigrew, G. W., & Seilman, S. (1982) *Biochem. J. 201*, 9-18.
Poulos, T. L., & Kraut, J. (1980) *J. Biol. Chem. 255*, 10322-10330.
Poulos, T. L., & Mauk, A. G. (1983) *J. Biol. Chem. 258*, 7369-7373.
Przysiecki, C. T., Bhattacharyya, A., Tollin, G., & Cusanovich, M. A. (1985a) *J. Biol. Chem. 260*, 1452-1458.
Przysiecki, C. T., Tollin, G., Meyer, T. E., Staggers, J. E., & Cusanovich, M. A. (1985b) *Arch. Biochem. Biophys. 238*, 334-343.
Rees, D. C. (1985) *Proc. Natl. Acad. Sci. U.S.A. 82*, 3082-3085.
Salemme, F. R. (1976) *J. Mol. Biol. 102*, 563-568.
Salemme, F. R. (1978) *Annu. Rev. Biochem. 46*, 299-329.
Simondsen, R. P., & Tollin, G. (1983) *Biochemistry 22*, 3008-3016.
Simondsen, R. P., Weber, P. C., Salemme, F. R., & Tollin, G. (1982) *Biochemistry 21*, 6366-6375.
Strickland, S., Palmer, G., & Massey, V. (1975) *J. Biol. Chem. 250*, 4048-4052.
Sutin, N. (1983) *Prog. Inorg. Chem. 30*, 441-498.
Tainer, J. A., Getzoff, E. D., Sayre, J., & Olson, A. J. (1985) *J. Mol. Graphics 3*, 103-105.
Tollin, G., Cheddar, G., Watkins, J. A., Meyer, T. E., & Cusanovich, M. A. (1984) *Biochemistry 23*, 6345-6349.
Vaish, S. P., & Tollin, G. (1971) *Bioenergetics 2*, 61-72.
Waldmeyer, B., & Bosshard, H. R. (1985) *J. Biol. Chem. 260*, 5184-5190.
Waldmeyer, B., Bechtold, R., Bosshard, H. R., & Poulos, T. L. (1982) *J. Biol. Chem. 257*, 6073-6076.
Weber, P. C., & Tollin, G. (1985) *J. Biol. Chem. 260*, 5568-5573.
Wilson, G. S. (1978) *Methods Enzymol. 54E*, 396-410.

Spectroscopic Properties of the Cobalt(II)-Substituted α-Fragment of Rabbit Liver Metallothionein†

Meinrad Good and Milan Vašák*
Biochemisches Institut der Universität Zürich, CH-8057 Zürich, Switzerland
Received November 19, 1985; Revised Manuscript Received January 28, 1986

ABSTRACT: The C-terminal segment of rabbit liver metallothionein 1 (α-fragment) containing four paramagnetic Co(II) ions was obtained by stoichiometric replacement of the originally bound diamagnetic Cd(II) ions. The latter form was prepared by limited proteolysis with subtilisin as described previously [Winge, D. R., & Miklossy, K. A. (1982) *J. Biol. Chem. 257*, 3471-3476]. Electronic absorption, magnetic circular dichroism (MCD), and electron paramagnetic resonance (EPR) measurements were employed to monitor the stepwise incorporation of Co(II) ions into the metal-free fragment. Absorption and MCD spectra of the apofragment containing the first 3 Co(II) equiv show the typical features of tetrahedral tetrathiolate Co(II) coordination. However, in the d-d region only small changes in the visible and no apparent change in the near-infrared region are discernible when the fourth Co(II) is bound. This unusual spectral behavior was not seen in Co(II) substitution of native metallothionein [Vašák, M., & Kägi, J. H. R. (1981) *Proc. Natl. Acad. Sci. U.S.A. 78*, 6709-6713] and may indicate a different cluster geometry. In the charge-transfer region, the binding of all 4 Co(II) equiv is accompanied by characteristic increments of the thiolate S→Co(II) bands. As in the formation of $Co(II)_7$-metallothionein, the development of the the charge-transfer and EPR spectral properties upon binding of the first 2 Co(II) equiv to the apofragment is indicative of isolated, noninteracting tetrahedral tetrathiolate Co(II) complexes. The binding of the additional Co(II) ion is accompanied by a red shift in the charge-transfer region and by the dramatic loss of paramagnetism in the EPR spectra, both diagnostic of the formation of metal-thiolate cluster structures. Thus, these data suggest that the four-metal cluster in the isolated α-fragment and in $Co(II)_7$-metallothionein is similar but not identical.

Metallothioneins represent a class of low molecular weight metal and sulfur-rich proteins, which are widely distributed in nature (Kägi et al., 1984). An interesting feature of all these proteins is that their biosynthesis can be induced by the administration a variety of agents, among them heavy metals. It is therefore believed that metallothioneins are involved in trace metal metabolism and storage and detoxification of essential and nonessential d^{10} metal ions (Nordberg & Kojima, 1979). All mammalian forms examined to date consist of a single polypeptide chain with 61 amino acids of which 20 residues are cysteine and contain seven diamagnetic metal ions such as Zn(II) and/or Cd(II). There are two major electrophoretically separable isoforms present in most mammals, metallothioneins 1 and -2, that have closely related but distinct amino acid sequences (Kägi et al., 1984).

Spectroscopic studies have established that metallothioneins have a well-defined tertiary structure in which each metal ion is tetrahedrally coordinated by four thiolate ligands (Vašák et al., 1981) and that these metals are arranged in two separate clusters of three and four metals, respectively (Otvos & Ar-

† This work was supported by Swiss National Science Foundation Grant 3.146-085.
* Address correspondence to this author.

0006-2960/86/0425-3328$01.50/0

mitage, 1980). This cluster architecture is supported by the demonstration that native metallothionein can be cleaved by proteolytic digestion into two half-molecules (Winge & Miklossy, 1982; Nielson & Winge, 1984). The latter studies also indicated that the four-metal cluster (α-fragment) is formed by the C-terminal part, whereas the three-metal cluster (β-fragment) is made up of the N-terminal part of the polypeptide chain.

Although the available spectroscopic information on the structural characteristics of metallothionein is now substantial, it reflects in most cases the sum of the unresolved contributions of both clusters present in the native protein. The only two spectroscopic studies on record dealing with isolated clusters are the ^{113}Cd NMR measurements of the α-fragment from rat liver metallothionein, which revealed four ^{113}Cd resonances with chemical shifts comparable to those found in Cd_7–metallothionein (Boulanger et al., 1982), and the circular dichroism and magnetic circular dichroism measurements of the cadmium-containing form (Zelazowski et al., 1984). The aim of this work was to explore in more detail the structural properties of the four-metal fragment and to compare them with the corresponding features of the uncleaved protein. For this purpose, we have isolated the α-fragment of rabbit liver metallothionein 1 and examined the spectroscopic properties of its Co(II) derivative. The substitution of diamagnetic Zn(II) by paramagnetic Co(II) ions in a number of metalloproteins (Holmquist et al., 1975; Vallee & Holmquist, 1980) has provided valuable information about the geometry of the metal binding sites. In this study, the coordination geometry of the metal binding sites of the C-terminal cluster and its mode of formation are examined by electronic absorption, magnetic circular dichroism (MCD),[1] circular dichroism (CD), and electron paramagnetic resonance (EPR) techniques. Our results provide evidence for a T_d-type symmetry in the binding of the first three Co(II) ions. The different spectroscopic features associated with the binding of the fourth Co(II) ion imply a different coordination geometry for this metal binding site.

Materials and Methods

Chemicals and Instruments. Rabbit liver metallothionein was isolated from rabbits injected with $CdCl_2$ by 20 subcutaneous injections of 1 mg of cadmium sulfate/kg of body weight at intervals of 2–3 days. Metallothionein was purified by a combination of the procedures of Kimura et al. (1979) and Kägi et al. (1974). The purity of each preparation was examined by amino acids analysis (Durum D-500) and by metal analysis with atomic absorption spectrometry (Instrumentation Laboratory IL 157). All studies reported in this paper were performed on the isoform metallothionein 1. All inorganic and organic chemicals were of reagent grade or better, and prepared solutions were stored in polyethylene bottles. Subtilisin Carlsberg from *Bacillus subtilis* was from Fluka. Absorption spectra were recorded on a Perkin-Elmer Model 340 spectrophotometer in 1.0- and 0.1-cm quartz cells. The spectra in the near-infrared region were obtained in solutions of D_2O (99.5%). Molar absorptivities ϵ are given in units of M^{-1} cm^{-1}. EPR measurements were performed at a temperature of 3.4K, on a Varian E 112 spectrometer, operating in the X-band mode. EPR spectra were quantitated by the method of double integration (Palmer, 1967). A Jasco spectropolarimeter (Model J-500), connected on-line with an Epson-QX personal computer, was used for MCD and CD measurements, employing a constant magnetic field of 15 kG at room temperature. For each measurement the field was set parallel and antiparallel in the direction of the light beam, in order to improve the signal to noise ratio. MCD and CD curves were calculated as follows: for measurements of the magnetic field parallel to the propagation of the light beam

$$\Delta E(+) = \Delta E(\mathrm{CD}) + H\Delta E(\mathrm{MCD})$$

and for those for the antiparallel direction

$$\Delta E(-) = \Delta E(\mathrm{CD}) - H\Delta E(\mathrm{MCD})$$

where $\Delta E(+)$ and $\Delta E(-)$ are the observed differences in absorbance of left and right circular polarized light for parallel (+) and antiparallel (−) directions of the magnetic field H, respectively. Taking the difference of the two observed spectra cancels the CD component and leaves the MCD at twice the intensity of a single measurement. Addition of the two observed spectra yields twice the CD spectrum. Molar ellipticities $[\theta]_M$ and $[\theta]$ are given in units of deg cm^2 $dmol^{-1}$ G^{-1} and deg cm^2 $dmol^{-1}$, respectively.

Preparation of Apometallothionein. Apometallothionein, the metal-free protein, was prepared by gel filtration of the native form at low pH. A neutral solution of Zn,Cd–metallothionein was adjusted to pH 1 and subsequently passed over a Sephadex G-25 column, equilibrated with 0.01 N HCl. Protein concentration was determined spectrophotometrically by measuring the absorbance of apometallothionein in 0.01 N HCl at 220 nm with an extinction coefficient of 48 200 M^{-1} cm^{-1} (Bühler & Kägi, 1979).

Preparation of α-Fragment. The procedure of Winge and Miklossy (1982) was used with minor modifications. Prior to subtilisin cleavage, 2 mL of 1.25 mM apometallothionein (15 mg) in 0.01 N HCl was used for partial reconstitution with 4 equiv of $CdCl_2$. Subsequently, this solution was diluted with 3 mL of 10 mM potassium phosphate buffer (pH 7.6) and the pH adjusted to 7.6 with 1 N KOH. A total of 100 μL of a freshly prepared solution of subtilisin (2 mg/mL) in the same buffer was then added and the sample incubated at 4 °C for about 15 h. In order to minimize oxidation of cysteine sulfur, all solutions were saturated prior to use with nitrogen, and all preparative steps were carefully performed in a N_2-purged glovebox. Subsequently, the sample was concentrated to about 1.5 mL by ultrafiltration (Amicon apparatus, YM2 membrane) and separated over a Sephadex G-75 superfine column (150 × 1.5 cm), equilibrated with 10 mM phosphate buffer, pH 7.6, at 4 °C. The elution profile consisted of two well-separated peaks with an elution coefficient K_D of 0.51 and 0.68, respectively. On the basis of the amino acid composition and N-terminal amino acid determination (De Jong et al., 1982), the peak with $K_D = 0.68$ contained the C-terminal fragment of rabbit liver metallothionein 1 (residues 31–61) starting with Lys-31. The preparative yield in nine independent preparations ranged between 35 and 40%. The metal-free peptide (apo-fragment) was prepared similarly to apometallothionein (see above). Prior to metal reconstitution, all 11 cysteine residues were determined with Ellman's reagent (DTNB) in 10 mM potassium phosphate buffer, pH 7.5 (ϵ_{412} = 13 600 M^{-1} cm^{-1}) (McGilvray & Morris, 1971). On the basis of quantitative amino acid analysis, the molar extinction coefficient of the α-fragment at 220 nm in 0.01 N HCl was found to be 32 400 M^{-1} cm^{-1}.

Preparation of Co(II)–Fragment. All solutions used in the preparation of the Co(II)–fragment were degassed on a vacuum line prior to use, and the procedures were performed in

[1] Abbreviations: MCD, magnetic circular dichroism; CD, circular dichroism; EPR, electron paramagnetic resonance; T_d, tetrahedral; DTNB, 5,5′-dithiobis(2-nitrobenzoic acid); Tris, tris(hydroxymethyl)-aminomethane.

Table I: Amino Acid Composition of α-Fragment of Rabbit Liver Metallothionein 1

residue	analysis[a]	residue	analysis[a]
Cys[b]	11.11 (11)	Gly	3.49 (3)
Asx	1.13 (1)	Ala	3.77 (4)
Thr	1.06 (1)	Ile	0.89 (1)
Ser	3.74 (4)	Lys	3.93 (4)
Glx	1.15 (1)		
Pro	0.72 (1)	total residues	31

[a] The amino acid analysis was performed after performic acid oxidation (16 h at 0 °C) and hydrolysis (20 h at 110 °C) in 6 N HCl. [b] Analyzed as cysteic acid.

an argon-purged glovebox (Vašák et al., 1981). A freshly prepared solution of 0.2 mM apofragment in 0.1 N HCl was mixed with 50 mM $CoSO_4$ in bidistilled water, yielding the desired metal to protein ratio. The solution mixture was then adjusted to pH 8.3 by the addition of 2 equiv of 1 M Tris base (Trizma from Sigma). The metal to fragment ratios were determined independently with a small aliquot of the sample. The green Co(II) complex is highly oxygen sensitive and yields a light brown product upon exposure to air.

Results and Discussion

The ability of the C-terminal fragment of rat liver metallothionein to bind four diamagnetic Cd(II) ions was demonstrated by Winge and Miklossy (1982). In this study, the same metal to protein stoichiometry was confirmed also in the isolated α-fragment of rabbit liver metallothionein. The amino acid composition of this isolated α-fragment is shown in Table I. By the replacement of the diamagnetic Cd(II) ions with paramagnetic Co(II) ions, a $Co(II)_4$–fragment was obtained (see below). This reconstituted $Co(II)_4$–fragment was subjected to detailed spectroscopic studies. The first part of this paper presents electronic absorption, CD, and MCD spectra in the visible and high-energy region of the fully metal occupied $Co(II)_4$–fragment and compares them with those of $Co(II)_7$–metallothionein (dashed lines in Figures 1 and 2). The second part deals with the formation of the tetranuclear cluster as monitored by electronic absorption, MCD, and EPR measurements.

Spectral Properties of $Co(II)_4$–Fragment. (A) Visible Region of $Co(II)_4$–Fragment. Figure 1 shows the electronic absorption, MCD, and CD spectrum of the fully metal occupied $Co(II)_4$–fragment (solid lines) and $Co(II)_7$–metallothionein (dashed lines) under the same experimental conditions. The electronic absorption spectrum (Figure 1, top) of $Co(II)_4$–fragment reveals two bands with maxima at 738 and 685 nm and a shoulder near 620 nm with molar absorptivities of 350, 390, and 280 M^{-1} cm^{-1}, respectively. These features are typical of tetrahedral Co(II)–thiolate coordination and closely resemble those reported for inorganic tetrathiolate–Co(II) complexes (Anglin & Davison, 1975; Holah & Coucouvanis, 1975; Lane et al., 1977; Swenson et al., 1978; Dance, 1979) and for Co(II)-substituted metalloproteins with four cysteine ligands, for example, Co(II)–rubredoxin (May & Kuo, 1978) and horse liver alcohol dehydrogenase with Co(II) bound at the noncatalytic metal binding site (Maret et al., 1979). A similar d–d profile was also found in horse and rabbit liver $Co(II)_7$–metallothionein (Vašák, 1980; Vašák & Kägi, 1981; Vašák et al., 1981). Interestingly, the molar absorptivity per cobalt is about one-third lower in the $Co(II)_4$–fragment as compared with $Co(II)_7$–metallothionein (Table II). The resolved d–d band pattern can be assigned to the spin-allowed and symmetry-forbidden $\nu_3[^4A_2 \rightarrow {}^4T_1(P)]$ transition. The four most intense peaks of Co(II) in the crystal

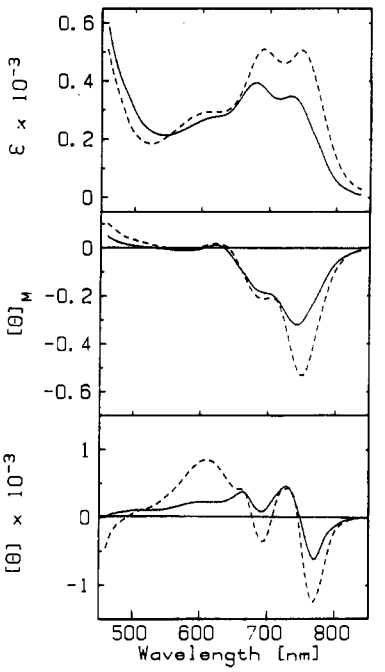

FIGURE 1: Absorption (top), MCD (middle), and CD (bottom) spectra of 0.17 mM $Co(II)_4$–fragment (solid lines) and 0.17 mM $Co(II)_7$–metallothionein (dashed lines) in 160 mM Tris-HCl, pH 8.3 at room temperature. ε, $[\theta]_M$, and $[\theta]$ are based on the concentration of Co(II). (For details, see Materials and Methods.)

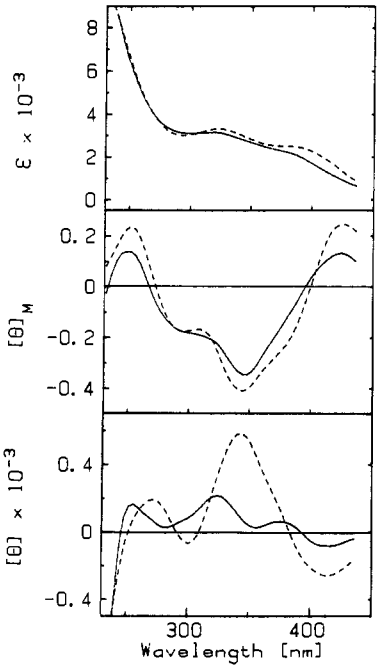

FIGURE 2: Absorption (top), MCD (middle), and CD (bottom) spectra of the $Co(II)_4$–fragment (solid lines) and $Co(II)_7$–metallothionein (dashed lines). ε, $[\theta]_M$, and $[\theta]$ are based on the concentration of Co(II). Conditions are as in Figure 1.

lattice of ZnS or CdS were shown to originate from the ν_3 transition to the $^4T_1(P)$ excited state split by spin–orbit coupling into four sublevels E′, $^3/_2$ U′, E″, and $^5/_2$ U′ (Weakliem, 1962). In the absorption spectrum of the $Co(II)_4$–fragment, only three spin–orbit coupling components with an energy separation of 1050 and 1530 cm^{-1} are clearly resolved (Figure 1, top). This energy separation is smaller than that obtained with fully metal occupied rabbit liver $Co(II)_7$–metallothionein of 1146 and 2175 cm^{-1} (Vašák et al., 1981) and is larger than that to be expected from spin–orbit coupling alone (Cotton

Table II: Comparison of Electronic Absorption, MCD, and CD Maxima of Fully Metal Occupied $Co(II)_4$–Fragment and $Co(II)_7$–Metallothionein (in Parentheses)

absorption		MCD		CD	
nm	ϵ ($\times 10^{-3}$)[a]	nm	$[\theta]_M$[a]	nm	$[\theta]$ ($\times 10^{-3}$)[a]
1272 (1275)	0.11 (0.16)				
738 (748)	0.35 (0.51)	743 (750)	−0.330 (−0.550)	768 (768)	−0.715 (−1.247)
				728 (732)	0.465 (0.530)
685 (690)	0.39 (0.51)	695, sh (688)	−0.192 (−0.222)	690 (695)	0.044 (−0.332)
		617 (616)	0.006 (0.004)	663 (662, sh)	0.393 (0.477)
620, sh (600, sh)	0.28 (0.29)	573 (572)	−0.001 (−0.021)	600, sh (610)	0.262 (0.924)
				500	0.103
390, sh (390, sh)	2.14 (2.44)	427 (426)	0.127 (0.250)	415 (417)	−0.800 (−2.615)
320 (320)	3.18 (3.33)	347 (345)	−0.332 (−0.414)	375	0.670
		290, sh (290, sh)	0.179 (0.174)	324 (343)	2.400 (5.928)
		255 (255)	0.095 (0.261)	255 (275)	2.000 (2.040)

[a] Values are calculated per cobalt atom.

et al., 1961). The presence of the $\nu_2[^4A_2 \rightarrow {}^4T(F)]$ transition in the near-infrared region (Figure 4) at 1275 nm, also reported in $Co(II)_7$–metallothionein (Vašák et al., 1981), offers additional proof for tetrahedral coordination of at least some Co(II) ions in the fragment (see below).

Evidence for tetrahedral coordination is provided also by MCD measurements (Figure 1, middle). The ν_3 transition of the $Co(II)_4$–fragment in the visible region between 850 and 450 nm displays a strong negative MCD band at 743 nm with a pronounced shoulder near 690 nm and small positive and negative MCD bands at 617 and 573 nm, respectively. The positions of the first three low-energy MCD bands coincide with those of the resolved spin–orbit coupling components in the electronic absorption spectrum (Figure 1, top). Comparison of our MCD profile with those of well-defined Co(II) complexes of different coordination number and geometry (Kaden et al., 1974) denotes the existence of T_d-type symmetry at the metal binding site of the fragment. Similar MCD features have also been found in a number of tetrahedral and pseudotetrahedral Co(II) complexes (Katô & Akimoto, 1974). The MCD features arise most likely from the temperature-dependent C-term, whose origin lies in differing populations among the Zeeman sublevels in the ground state $^4A_2$ (Denning & Spencer, 1969; Schatz, 1970). The molar magnetic ellipticity $[\theta]_M$ at 740 nm, when calculated per Co(II) ion bound, yields a value that is about 40% lower in the case of the $Co(II)_4$–fragment than that found with $Co(II)_7$–metallothionein (Table II). A similar decrease in intensity was also found in the corresponding absorption band (see above). The possible cause for this intensity drop is discussed in the second part of this paper (see below).

The low-energy CD spectrum of $Co(II)_4$–fragment (Figure 1, below) displays a negative band at 768 nm and three positive bands at 728, 663, and near 600 nm with molar elipticities $[\theta]$ of 2860, 1860, 1570, and 1050 deg cm^2 dmol^{-1}, respectively. The CD spectrum, in marked contrast to the MCD spectrum, is very sensitive to conformational and vicinal changes at the metal binding site and, hence, provides less unambiguous information about the coordination geometry (Vallee & Holmquist, 1980). Again, the CD bands of the $Co(II)_4$–fragment differ quite appreciably from those of $Co(II)_7$–metallothionein. The CD bands associated with the d–d transition of the fragment are about half as intense.

(B) High-Energy Region of $Co(II)_4$–Fragment. Since apometallothionein does not absorb appreciably above 250 nm (Vašák & Kägi, 1983), all spectral features of the Co(II)-substituted fragment must arise from metal binding. Thus, the electronic absorption features (Figure 2, top) below the d–d region must be attributed either to charge-transfer transitions or to ligand internal excitations (Mastropolo et al., 1977) affected by the interaction with the metal ion. The electronic absorption spectrum of the fully metal occupied fragment displays a shoulder near 390 nm and a maximum at 320 nm with molar extinction coefficients of 1925 M^{-1} cm^{-1} and 3180 M^{-1} cm^{-1}, respectively. The 320-nm absorption band with molar absorptivity of about 1150 M^{-1} cm^{-1} per Co(II) thiolate bound was also seen in Co(II)-substituted forms of rubredoxin (May & Kuo, 1978), horse liver alcohol dehydrogenase (Drum & Vallee, 1970; Maret et al., 1979), and model complexes (Lane et al., 1979). The band is held to be diagnostic of the thiolate charge-transfer excitation CysS→Co(II) (Tennent & McMillin, 1979). A comparison of the molar absorptivities of the $Co(II)_4$–fragment in the charge-transfer region with those of $Co(II)_7$–metallothionein reveals that in contrast to the d–d and near-infrared region where marked differences are discerned (see above) the charge-transfer regions are almost identical. A higher resolution of this spectral region is provided by the corresponding MCD and CD spectra (Figure 2, middle and bottom). The MCD spectrum of the high-energy region displays two MCD bands of opposite sign at +427 and −347 nm and a shoulder near −290 nm and a maximum at +255 nm. The MCD bands of the $Co(II)_4$–fragment and $Co(II)_7$–metallothionein are at the same positions but differ in the magnitude of ellipticity. The CD spectrum of $Co(II)_4$–fragment appears even better resolved than the corresponding MCD spectrum and is characterized by a number of ellipticity bands with maxima at −415, +375, +324, and +255 nm (Table II). The resolved CD profile of the $Co(II)_4$–fragment resembles that of $Co(II)_7$–metallothionein, but its amplitude per Co(II) ion is markedly diminished. A possible explanation for this effect is the increased symmetry of the Co(II) sites in the $Co(II)_4$–fragment suggested also by the decreased energy separation of the spin–orbit coupling components of the ν_3 transition (see above). On the basis of the comparison between the tetrahedrally coordinated $Co(II)_7$– and $Ni(II)_7$–metallothionein derivatives, all three low-energy CD bands in both metal derivatives were assigned to S→Me(II) excitations (Vašák et al., 1981). Hence, it is inferred that the same assignment holds also for the first three low-energy CD bands in the $Co(II)_4$–fragment.

Cluster Formation. To gain insight into the pathway of metal incorporation and cluster formation, the changes in the electronic absorption, MCD, and EPR spectra were monitored upon incremental additions of Co(II) to the apofragment. The electronic absorption features emerging in the charge-transfer region are shown in Figure 3 (left). In spite of the apparent similarity of the various profiles, there are distinct changes attending the increase of metal occupancy. Upon the addition of the first 2 Co(II) equiv to the apofragment, the absorption envelope reveals two rather well-resolved charge-transfer

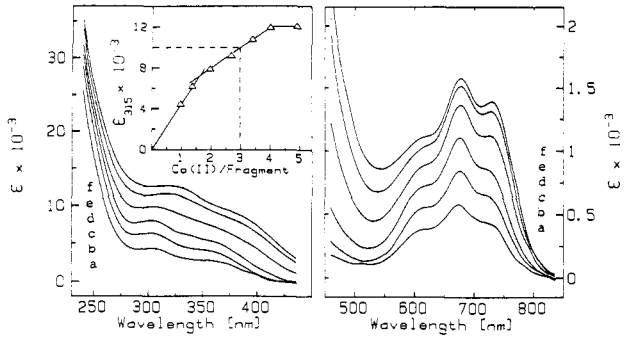

FIGURE 3: (Left) Absorption spectra in the charge-transfer region of the Co(II)–fragment as a function of Co(II) to protein ratio. The moles of Co(II) per mole of apofragment ratio is: (a) 1.0, (b) 1.5, (c) 2.1, (d) 2.7, (e) 3.4, and (f) 4.0. (Inset, left) Dependency of the absorbance at 315 nm on the Co(II) to protein ratio. (Right) Absorption spectra in the d–d region of the Co(II)–fragment as a function of Co(II) to protein ratio. The moles of Co(II) per mole of apofragment ratio is (a) 1.0, (b) 1.5, (c) 2.1, (d) 2.7, (e) 3.4, and (f) 4.0. ϵ is based on the protein concentration. Conditions are as in Figure 1.

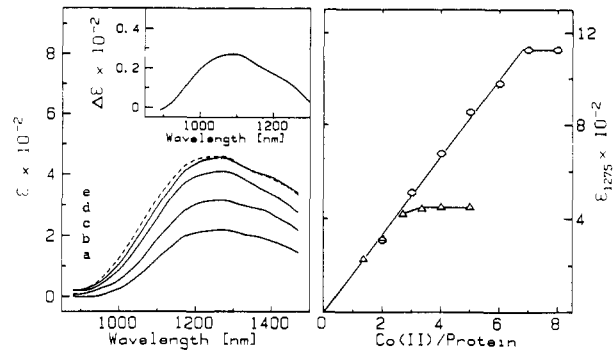

FIGURE 4: (Left) Absorption spectra in the near-infrared region of the Co(II)–fragment (0.17 mM) in D_2O (160 mM Tris-DCl, pD 8.3) as a function of Co(II) to protein ratio. The moles of Co(II) per mole of apofragment ratio is (a) 1.3, (b) 2.0, (c) 2.7, (d) 3.4, and (e) 4.0. (Inset, left) Difference absorbance spectrum of spectrum d vs. e. (Right) Dependency of the absorbance at 1275 nm as a function of Co(II) to protein ratio of the Co(II)–fragment (Δ) and Co(II)–metallothionein (O). ϵ is based on the protein concentration.

maxima at 305 and 350 nm. The subsequent addition of the remaining 2 Co(II) equiv results in a bathochromic shift of these maxima to 320 and 390 nm, respectively. Further addition of Co(II) ions to the $Co(II)_4$–fragment does not affect the spectrum. Differences comparable to those observed between the partially and fully metal saturated Co(II)–fragment have also been observed by Dance (1979) in the spectra of crystallographically defined tetrahedral thiolate complexes of mononuclear and tetranuclear Co(II)–benzenethiolate, i.e., $[Co(SPh)_4]^{2-}$ and $[Co_4(SPh)_{10}]^{2-}$, respectively. While the former complex contains only terminal sulfur ligands, the latter complex is made up of four terminal and six bridging sulfurs. Thus, the red shift in the absorption spectrum of the $Co(II)_4$–fragment attending the filling up process must be due to the involvement of bridging thiolate sulfur in metal coordination and reflects probably the stronger polarization of the bridging thiolate ligands by the two adjacent metal ions. The participation of thiolate ligands in all complexes formed in titration with Co(II) is documented by an increase of the molar absorptivity followed at 315 nm as a function of increasing metal binding site occupation (Figure 3, inset). The change of the slope at about 1.7 Co(II) equiv from 4330 to 2150 reflects the transition from mononuclear complexes containing solely terminal thiolates to oligonuclear entities where the metals are connected by bridging thiolate ligands. Accepting that the molar extinction coefficient for all 11 Co(II)-coordinated thiolate sulfurs of the α-fragment is comparable ($\epsilon_{315} \approx 1150\ M^{-1}\ cm^{-1}$),[2] it follows from the initial slope that the first 1.7 Co(II) equiv must be coordinated by four terminal thiolate ligands. More direct evidence for the initial formation of such isolated T_d sites is provided also by EPR titration (see Figure 6, right). The decrease in slope setting in above 1.7 Co(II) equiv signals partial sharing of the ligands leading to a reduction in Co(II)-to-thiolate stoichiometry. Thus, on the basis of the same molar absorptivity for the thiolate sulfurs, binding of 3 Co(II) equiv to apofragment requires only nine ligands for metal coordination (see Figure 3, inset).

The effect of increasing Co(II) to apofragment ratios on the absorption spectrum in the visible region is shown in Figure 3 (right). The absorption features of the Co(II)–fragment occupied incompletely by Co(II) ions resemble those of the fully metal occupied $Co(II)_4$–fragment and are typical of a tetrahedral tetrathiolate coordination. The same conclusion can be drawn from the corresponding MCD and EPR spectra (Figures 5 and 6). However, there are also some distinct spectral changes developing with the filling up of the metal binding sites by Co(II) ions. Up to binding of about 2 equiv of Co(II), the d–d profile increases in intensity without changing shape. Addition of the remaining 2 Co(II) equiv to the apofragment alters the positions of the spin–orbit coupling components of the ν_3 transition. This is reflected in the shifts from 630, 680, and 725 nm to 620, 685, and 738 nm, respectively, resulting in increased energy separation between the corresponding spin–orbit coupling components from 1170 and 910 cm^{-1} to 1530 and 1050 cm^{-1}, respectively. It is possible that a part of these sites is influenced by the red shift of the charge-transfer bands that develops above 1.7 equiv of Co(II) and that leads to an overlap with the absorption profile in the visible region. However, the greater spacing of the two low-energy bands is clearly unaffected by such effects.

To get more information about the last metal binding site, the same stepwise incorporation of Co(II) ions was studied by monitoring the electronic absorption changes in the near-infrared region (Figure 4). Measuring the absorbance at 1275 nm, a linear increase is observed up to 3 equiv of Co(II) added (Figure 4, right). Addition of the fourth Co(II) equivalent produces no further change in absorbance at this spectral position. However, a slight increase in absorption is discerned at the high-energy edge of the spectral envelope. The difference between the last two titration steps yields a difference spectrum with a maximum near 1100 nm and a difference molar extinction coefficient of about 35 $M^{-1}\ cm^{-1}$ per Co(II) ion (Figure 4, inset). The about 5 times lower absorption increment upon addition of the last Co(II) is suggestive of a metal binding site of nontetrahedral symmetry. Further support for a different metal binding site in the Co(II) fragment comes from MCD studies (Figure 5). The MCD profiles resulting from the addition of the first three Co(II) resemble that of the fully metal saturated $Co(II)_4$–fragment and are typical of T_d-type symmetry (Figure 5). On the basis of a qualitative and quantitative comparison between the MCD profiles of Co(II)-substituted proteins and those of Co(II) model complexes, the coordination geometry can be deduced (Vallee & Holmquist, 1980). Thus, the MCD spectra generated by the addition of the first 3 equiv of Co(II) ions are

[2] Co(II) ions in $Co(II)_1$–metallothionein, coordinated solely by terminal thiolate ligands, and those in $Co(II)_1Zn(II)_6$–metallothionein, where both terminal and bridging thiolates participate on metal binding, exhibit at 315 nm comparable molar absorptivity per sulfur (M. Good, unpublished results).

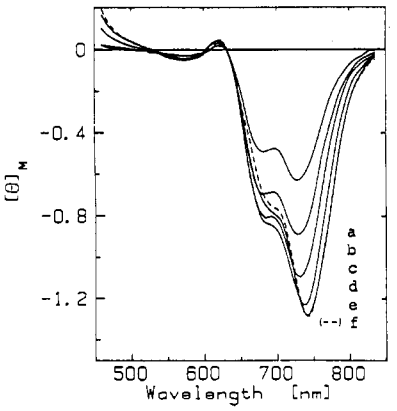

FIGURE 5: MCD spectra in the d–d region of the Co(II)–fragment as a function of metal to apofragment stoichiometry. The moles of Co(II) per mole of apofragment ratio is (a) 1.0, (b) 1.5, (c) 2.1, (d) 2.7, (e) 3.4, and (f) 4.0. $[\theta]_M$ is based on the protein concentration. Conditions are as in Figure 1.

typical of tetrahedral metal coordination. Pentacoordination would be characterized by the presence of two rather strong structured bands in MCD as well as in absorption. In contrast, the intensity of the absorption spectra of octahedral complexes (e.g., $[Co(H_2O)_6]^{2+}$) are generally low, $\epsilon = 4$–$10\ M^{-1}\ cm^{-1}$, and their MCD spectra are characterized by a slightly structured negative band centered at higher energy with a magnetic molar ellipticity $[\theta]_M$ of only –0.006 to –0.028 deg $cm^2\ dmol^{-1}\ G^{-1}$. Thus, the failure of the last Co(II) to elicit only minor increments in absorption and MCD in the d–d region might be compatible with its binding in an octahedral environment. Thus, for the latter coordination geometry additional non-sulfur ligands would be required. In order to probe the possibility of water coordination to the fourth metal binding site, the effect of I^- ions on the electronic absorption profile was examined up to a 35 molar excess of I^- over Co(II). In this case, no changes in the d–d as well as charge-transfer profiles were discerned, implying that additional non-sulfur ligands (e.g., oxygen) can be contributed only by the protein molecule.

The building up of the cluster was further studied with low-temperature (3.4K) EPR measurements. The EPR spectra of varying ratios of Co(II) to apofragment display qualitatively the same profiles but differ markedly in intensity. The spectrum of a sample with a metal to apofragment stoichiometry of 2.1 is shown in Figure 6 (left) and is typical of rhombically distorted high-spin Co(II) complexes with g values of $g_x \approx 5.7$, $g_y \approx 4.5$, and $g_z \approx 2.0$. Up to the binding of about 1.7 Co(II) equiv, the intensity of the signal at $g_x \approx 5.7$ increases linearly with Co(II) concentration. Beyond this ratio, the intensity drops, reaching a minimum at about 3 Co(II) equiv. This effect is attributable to antiferromagnetic coupling of vicinal tetrahedral tetrathiolate–Co(II) complexes sharing a common thiolate ligand and thus signals the emergence of the clustered structure in the fragment. The intensity drop in the EPR spectra parallels the red shift of the electronic absorption spectra in the charge-transfer region, which was attributed previously to the participation of bridging thiolates in metal binding (Vašák & Kägi, 1981). Reappearance of an EPR signal with comparable g values upon the addition of the last equivalent of Co(II) may be related to its somewhat different mode of binding. As suggested above, this Co(II) may be linked nontetrahedrally through bridging thiolate ligands to the nearly EPR-silent $Co(II)_3$ cluster and may reflect a perturbation of the antiferromagnetic exchange interactions within the $Co(II)_4$–fragment. Thus, the partial recovery of the EPR signal upon the addition of the fourth

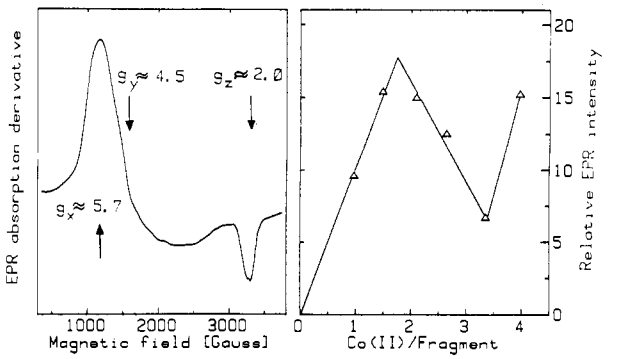

FIGURE 6: (Left) EPR spectrum of Co(II)–fragment containing 2.1 Co(II) per protein molecule. Conditions: 0.17 mM Co(II)–fragment in 160 mM Tris-HCl, pH 8.3; microwave power 0.8 mW; microwave frequency 9.236 GHz; 3.4K. (Right) Dependence of the EPR signal intensity on the Co(II) to protein ratio. Signal amplitude was calculated by employing the method of double integration.

Co(II) ion, which is not seen in $Co(II)_7$–metallothionein, is another indication of the nonidentity of the cluster structure in the holoprotein and the fragment. Recently, a similar reappearance of the amplitude of the EPR signal was observed for *Neurospora crassa* metallothionein when in addition to the 2 Co(II) equiv, coordinated in a binuclear tetrahedral tetrathiolate cluster, a third Co(II) ion was bound (Beltramini et al., 1984).

CONCLUSIONS

The spectroscopic studies presented here on the Co(II)-substituted α-fragment from rabbit liver metallothionein 1 extend our knowledge of the structure of the metal binding sites in this protein. The stepwise incorporation of the first 3 Co(II) equiv into the apofragment results in spectral features that confirm the prevalence of distorted tetrahedral tetrathiolate–Co(II) complexes. In fact, the essential preservation of the $\nu_3[^4A_2 \rightarrow {}^4T_1(P)]$ and $\nu_2[^4A_2 \rightarrow {}^4T_1(F)]$ transitions in the course of the filling up process indicates that this geometry applies to the first three metal sites to be occupied. In contrast, the occurrence of only a minor change in the ν_3 transition of the electronic absorption and in the MCD spectrum upon binding of the fourth Co(II) ion and the emergence of a new low-intensity difference band in the near-infrared region imply a different coordination geometry for this last metal site.

The examination of the electronic absorption, MCD, and EPR spectra at various stages of filling suggests that the first 2 Co(II) equiv go into completely noninteracting sites, each made up of four terminal thiolate ligands. As evidenced by the manifestation of antiferromagnetic coupling in the EPR behavior and the pronounced red shift in the charge-transfer region of the absorption spectra, the binding of the third Co(II) equivalent brings about cross-linking among the metal binding sites via bridging thiolate ligands. A tentative model compatible with all spectroscopic features of such a structure is a cyclic trinuclear metal–thiolate cluster with a ratio of three Co(II) to nine thiolate sulfurs:

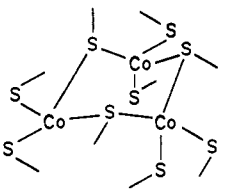

This structure resembles closely the NH_2-terminal three metal–thiolate cluster (cluster B) of mammalian metallothioneins proposed by Otvos and Armitage (1980). The same

model could allow the fourth metal to dock on the trinuclear metal–thiolate cluster, thereby forming an additional binding site of different coordination geometry.

Analogous differences between the α-fragment and the uncleaved protein are also seen in the Cd(II) derivatives. Titration of the apofragment with Cd(II) ions revealed CD features that are not observed in metal titration of apometallothionein (M. Good, unpublished results). Thus, the differences between the spectroscopic behavior of the α-fragment and that of metallothionein must be the result of protein cleavage. Consequently, it would appear that the N-terminal segment (β-fragment) of metallothionein is required to condition the formation of the C-terminal four-metal cluster in metallothionein.

Acknowledgments

We are indebted to Professor Dr. J. H. R. Kägi for his support throughout this work and for valuable discussions. We are grateful to Marietta Sutter for the preparation of metallothionein.

Registry No. S, 7704-34-9.

References

Anglin, J. R., & Davison, A. (1975) *Inorg. Chem. 14*, 234–237.

Beltramini, M., Lerch, K., & Vašák, M. (1984) *Biochemistry 23*, 3422–3427.

Boulanger, Y., Armitage, I. M., Miklossy, K. A., & Winge, D. R. (1982) *J. Biol. Chem. 257*, 13717–13719.

Bühler, R. H. O., & Kägi, J. H. R. (1979) in *Metallothionein* (Kägi, J. H. R., & Nordberg, M., Eds.) pp 211–220, Birkhäuser Verlag, Basel.

Cotton, F. A., Goodgame, D. M. L., & Goodgame, M. (1961) *J. Am. Chem. Soc. 83*, 4690–4699.

Dance, I. G. (1979) *J. Am. Chem. Soc. 101*, 6264–6273.

De Jong, C., Hughes, G. J., Van Wieringen, E., & Wilson, K. J. (1982) *J. Chromatogr. 241*, 345–359.

Denning, R. G., & Spencer, J. A. (1969) *Symp. Faraday Soc. 3*, 84–91.

Drum, D. D., & Vallee, B. L. (1970) *Biochem. Biophys. Res. Commun. 41*, 33–39.

Holah, D. G., & Coucouvanis, D. (1975) *J. Am. Chem. Soc. 97*, 6917–6919.

Holmquist, B., Kaden, T. A., & Vallee, B. L. (1975) *Biochemistry 14*, 1454–1461.

Kaden, T. S., Holmquist, B., & Vallee, B. L. (1974) *Inorg. Chem. 13*, 2585–2590.

Kägi, J. H. R., Himmelhoch, S. R., Whanger, P. D., Bethune, J. L., & Vallee, B. L. (1974) *J. Biol. Chem. 249*, 3537–3542.

Kägi, J. H. R., Vašák, M., Lerch, K., Gilg, D. E. O., Hunziker, P., Bernhard, W. R., & Good, M. (1984) *EHP, Environ. Health Perspect. 54*, 93–103.

Katô, H., & Akimoto, K. (1974) *J. Am. Chem. Soc. 96*, 1351–1357.

Kimura, M., Otaki, N., & Imano, M. (1979) in *Metallothionein* (Kägi, J. H. R., & Nordberg, M., Eds.) pp 163–168, Birkhäuser Verlag, Basel.

Lane, R. W., Ibers, J. A., Frankel, R. B., Papaefthymiou, G. C., & Holm, R. H. (1977) *J. Am. Chem. Soc. 99*, 84–98.

Maret, W., Anderson, I., Dietrich, H., Schneider, H., Einarsson, R., & Zeppezauer, M. (1979) *Eur. J. Biochem. 98*, 501–512.

Mastropolo, D., Tich, J. A., Potenza, J. A., & Schugar, H. J. (1977) *J. Am. Chem. Soc. 99*, 424–429.

May, W., & Kuo, J. Y. (1978) *Biochemistry 17*, 3333–3338.

McGilvray, D., & Morris, J. G. (1971) *Methods Enzymol. 17*, 585–589.

Nielson, K. B., & Winge, D. R. (1984) *J. Biol. Chem. 259*, 4941–4946.

Nordberg, M., & Kojima, Y. (1979) in *Metallothionein* (Kägi, J. H. R., & Nordberg, M., Eds.) pp 41–124, Birkhäuser Verlag, Basel.

Otvos, J. D., & Armitage, I. M. (1980) *Proc. Natl. Acad. Sci. U.S.A. 77*, 7094–7098.

Palmer, G. (1967) *Methods Enzymol. 10*, 594–609.

Schatz, P. N. (1970) *Q. Rev., Chem. Soc. 23*, 552–584.

Swenson, D., Baenziger, L. N., & Coucouvanis, D. (1978) *J. Am. Chem. Soc. 100*, 1932–1934.

Tennent, D. L., & McMillin, D. R. (1979) *J. Am. Chem. Soc. 101*, 2307–2311.

Vallee, B. L., & Holmquist, B. (1980) *Adv. Inorg. Biochem. 2*, 27–74.

Vašák, M. (1980) *J. Am. Chem. Soc. 102*, 3953–3955.

Vašák, M., & Kägi, J. H. R. (1981) *Proc. Natl. Acad. Sci. U.S.A. 78*, 6709–6713.

Vašák, M., & Kägi, J. H. R. (1983) *Met. Ions Biol. Syst. 15*, 213–273.

Vašák, M., Kägi, J. H. R., Holmquist, B., & Vallee, B. L. (1981) *Biochemistry 20*, 6659–6664.

Weakliem, H. A. (1962) *J. Chem. Phys. 36*, 2117–2140.

Winge, D. R., & Miklossy, K. A. (1982) *J. Biol. Chem. 257*, 3471–3476.

Zelazowski, A. J., Szymanska, J. A., Law, A. J. C., & Stillman, M. J. (1984) *J. Biol. Chem. 259*, 12960–12963.